Supporting Information

Carbonyl Functionalization Strategy to Solve the Easy Agglomeration Defect of Porphyrin

Mingli Li, Taotao Qiang[*]

College of Bioresources and Materials Engineering, Shaanxi Collaborative Innovation Center of Industrial Auxiliary Chemistry & Technology, Shaanxi University of Science & Technology, Xi'an, 710021, China.

*Corresponding author:

Taotao Qiang: qiangtt515@163.com

Table of Contents

Instrumentation and Materials

^{1}H NMR (600 MHz) spectra were recorded on a Bruker AVANCE NEO 600MHz spectrometer, and chemical shifts were reported using the delta scale in ppm relative to CHCl$_3$ as internal reference for ^{1}H NMR (δ = 7.260 ppm). Absorption spectra were recorded on a Cary 5000 spectrometer. MALDI-TOF mass spectra were obtained with a Bruker ultraflextreme MALDI-TOF/TOF spectrometer with matrix. Material surface morphology were observed on a FEI Verios 460 spectrometer. Dispersion of materials in aqueous solution were taken on an ALV/C spectrometer. Photogenic charge lifetime was recorded on an ultrafast systems helios spectrometer. Electrochemical data were measured by cyclic voltammetry on a PGSTAT 302N scanning electrochemical microscope. Free radical species were recorded on a CIQTEK EPR200-Plus spectrometer. Unless otherwise noted, materials obtained from commercial suppliers were used without further purification. **1** and **1Zn** were prepared according to the related literatures.[S1]

General Procedures
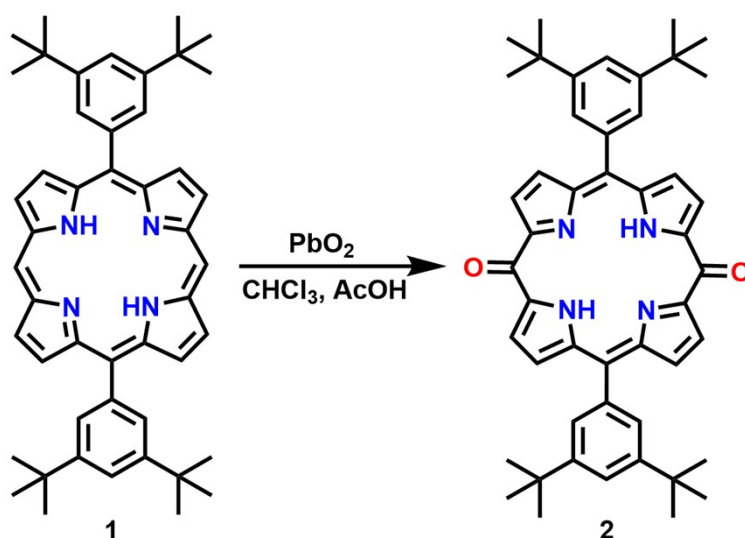
Synthesis of 2[S2]: Compound **1** (685 mg, 1.00 mmol) was dissolved in a mixture of chloroform (50 mL) and acetic acid (10 mL). PbO_2 (2.39 g, 10.0 mmol) was added and the reaction mixture was stirred for 5 h open to air, whereafter a saturated aqueous sodium bicarbonate solution (100 mL) was added slowly to neutralize acetic acid, and the organic phase was passed through a Celite pad to remove residual lead salts. The aqueous layer was extracted with dichloromethane, and the organic fraction was again passed through a Celite pad. The combined organic fraction was washed by water and dried with anhydrous Na_2SO_4. The solvent was removed in vacuo. The crude product was purified by column chromatography on silica gel

(petroleum ether/dichloromethane = 1/1) to give the desired product **2** (500 mg, 0.7 mmol, 70%) as red solid.
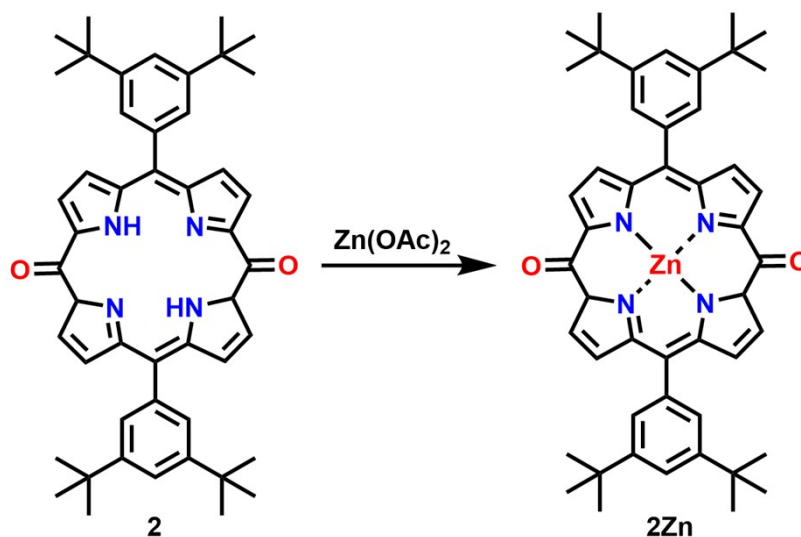
Synthesis of 2Zn[S1]: **2** (1.00 g, 1.40 mmol) was added to a round-bottomed 250 mL flask containing a magnetic stirring bar, and dissolved in CH_2Cl_2 (100 mL)/MeOH (10 mL). $Zn(OAc)_2$ (0.78 g, 4.20 mmol) was added, after being stirred at 25 ˚C for 3 h. The reaction mixture was poured in to water and the products were extracted with CH_2Cl_2. The organic extracts were combined, washed with water, and dried over anhydrous sodium sulfate. The solvent was evaporated, and the product was recrystallization with CH_2Cl_2/MeOH, **2Zn** (1.04 g, 1.33 mmol, 95% yield) was obtained as a red solid.

Photocatalytic process[S3]: The photocatalytic reduction of heavy metal

Cr(VI) was carried out in Xe lamp (1.0 W/cm^2, 320-2500 nm) irradiation. The effects of the amount of photocatalyst (5-40 mg), the concentration of Cr(VI) (10-60 mg/L), pH (2-8). The amount of Cr(VI) aqueous solution was 30mL, and the pH value was adjusted with 1M H_2SO_4 and 1M NaOH. After stirring in the dark for 30 min, the photocatalyst and Cr(VI) aqueous solution reached adsorption equilibrium, and the suspension was irradiated by Xe lamp. During the catalysis process, 2 mL suspension was collected at an interval of 30 min, and the suspended catalyst was removed with a stream filter (0.22μm). The content of Cr(VI) was determined by Agilent Cary 5000 UV-vis spectrophotometer at 540 nm.

Compounds Data

2: ^{1}H NMR (600 MHz, CDCl$_3$): δ = 13.55 (s, 2H), 7.52 (s, 2H), 7.34 (d, J = 27.6 Hz, 4H), 6.70 (d, J = 4.2 Hz, 4H), 6.53 (d, J = 4.2 Hz, 4H), 1.40 (s, 18H), 1.34 (s, 18H) ppm; HR-MS (MALDI-TOF-MS) m/z = 718.4168 [M]$^+$, calcd for (C$_{48}$H$_{54}$N$_4$O$_2$)$^+$ = 718.4247.

2Zn: ^{1}H NMR (600 MHz, CDCl$_3$): δ = 7.43 (d, J = 1.8 Hz, 2H), 7.08 (d, J = 1.8 Hz, 4H), 7.01 (d, J = 4.2 Hz, 4H), 6.22 (d, J = 4.2 Hz, 4H), 1.24 (s, 36H) ppm; HR-MS (MALDI-TOF-MS) m/z = 780.3347 [M]$^+$, calcd for (C$_{48}$H$_{52}$N$_4$O$_2$Zn)$^+$ = 780.3382; UV/Vis (CHCl$_2$): λ$_{max}$ (ε [M^{-1}cm^{-1}]) = 363 (47100), 451 (86900), 509 (20100), 546 (80400) nm.

NMR spectra
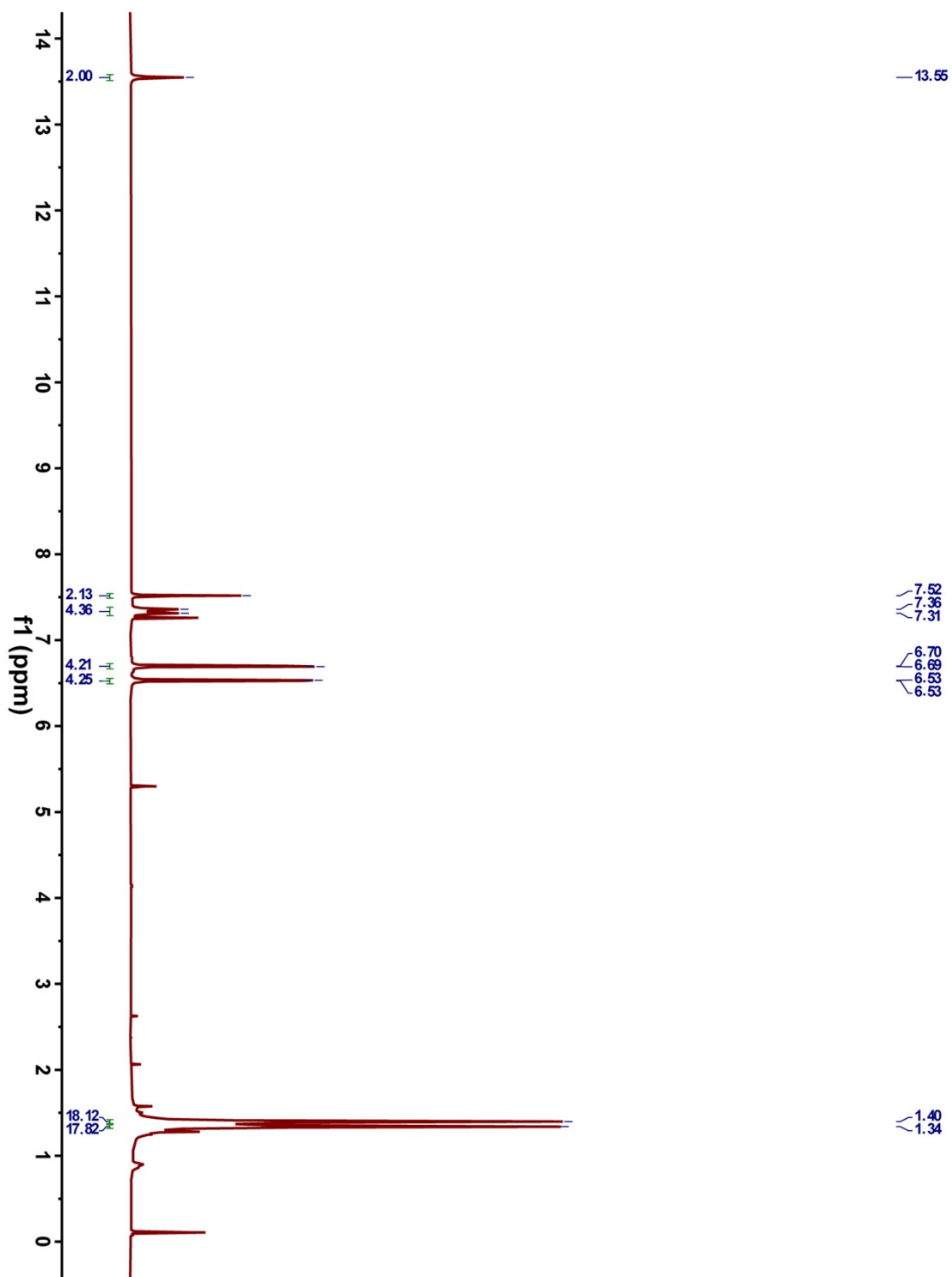
Figure S1. ^{1}H NMR spectrum of **2** in CDCl$_3$.
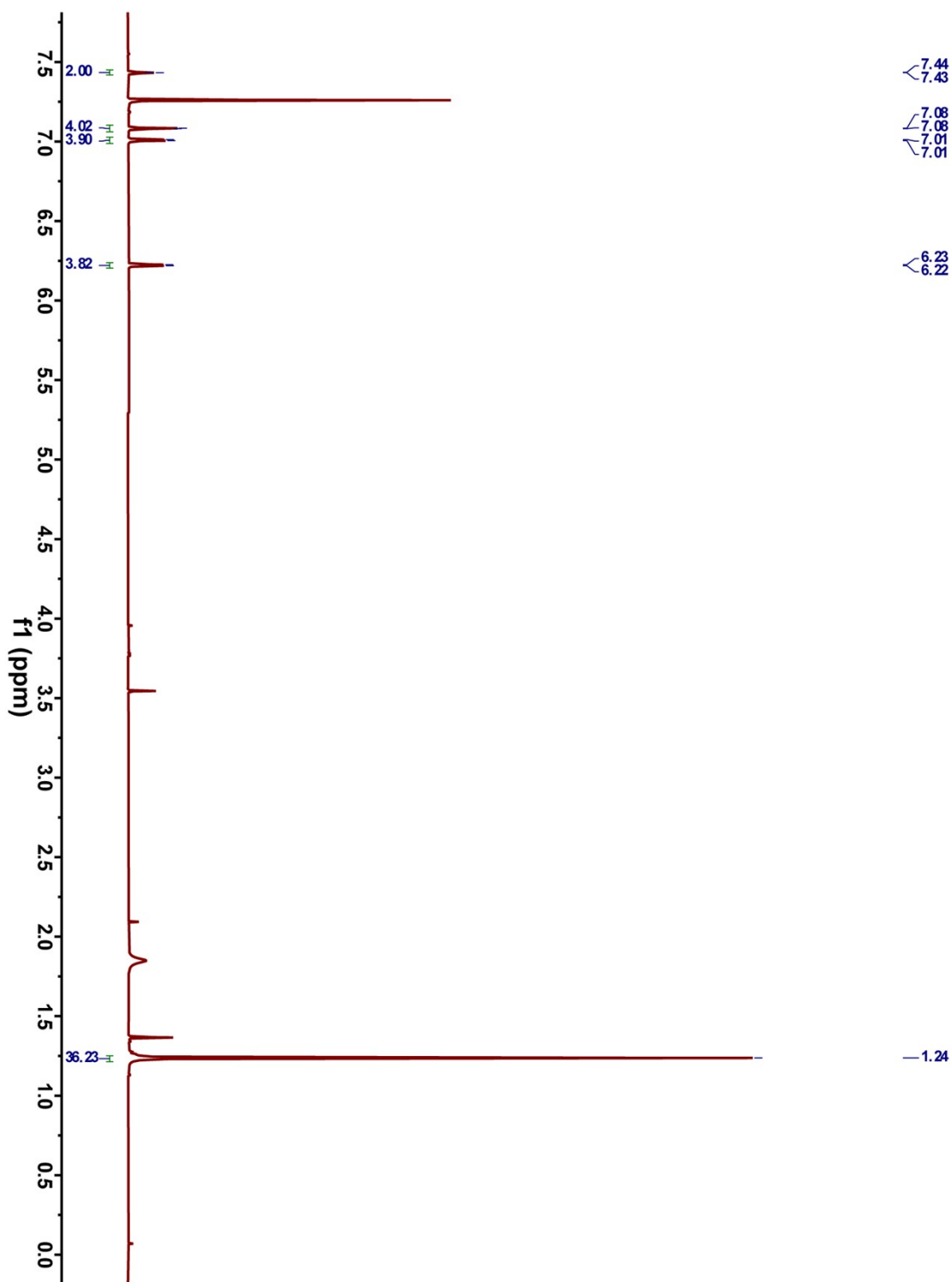
Figure S2. ¹H NMR spectrum of **2Zn** in CDCl₃.

Mass Spectra
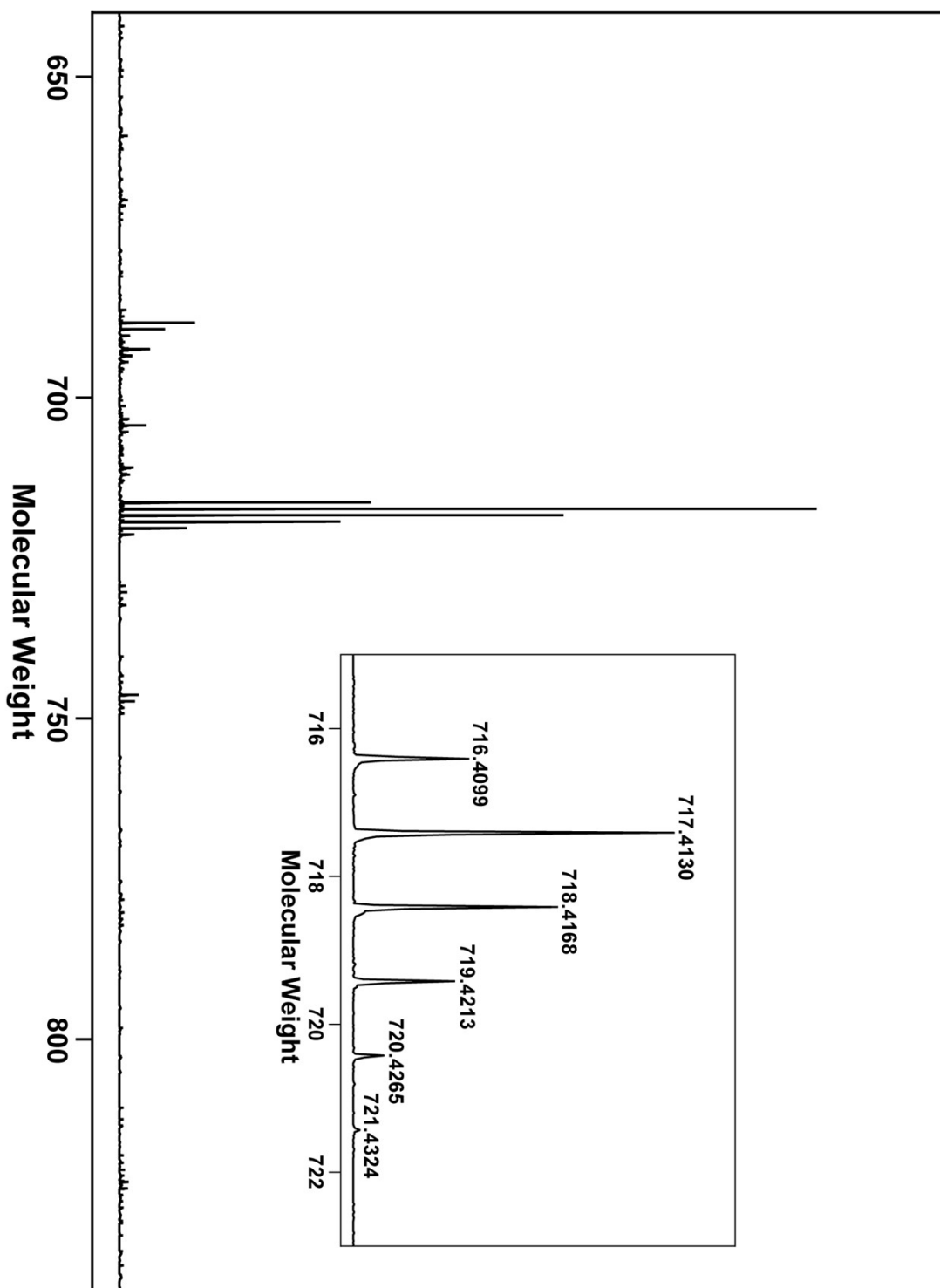
Figure S3. HR-MS spectrum of **2**.
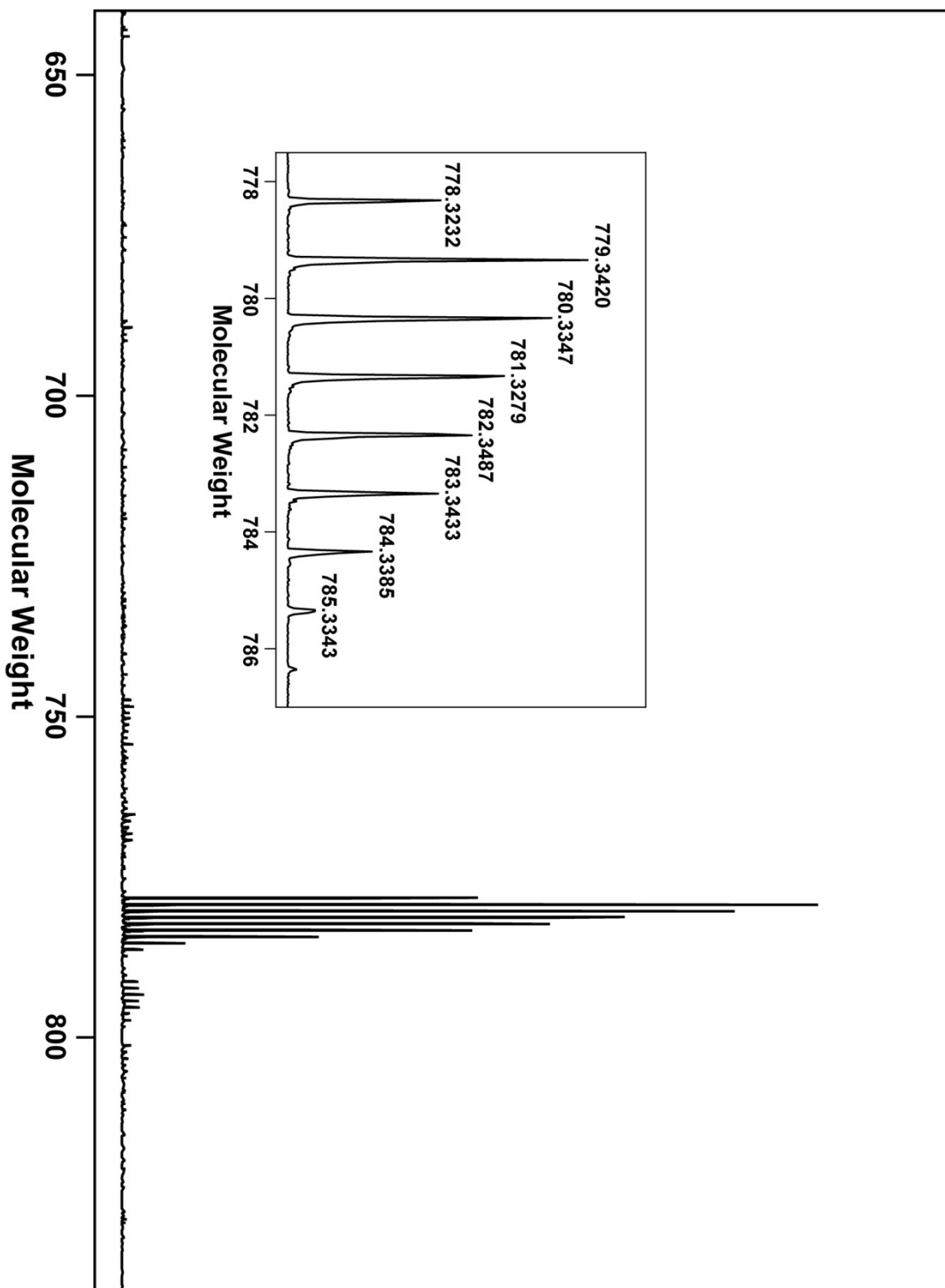
Figure S4. HR-MS spectrum of **2Zn**.

Application Experimental Data
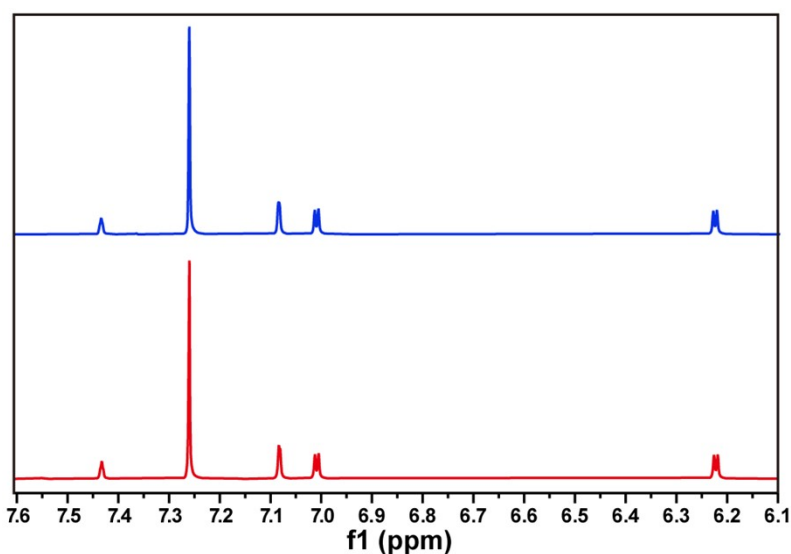
Figure S5. Schematic diagram of the verification of the stability of **2Zn** by ^{1}H-NMR spectra (red is the ^{1}H-NMR spectrum before the photocatalysis experiment, and blue is the ^{1}H-NMR spectrum after eight cycles of the photocatalysis experiment).
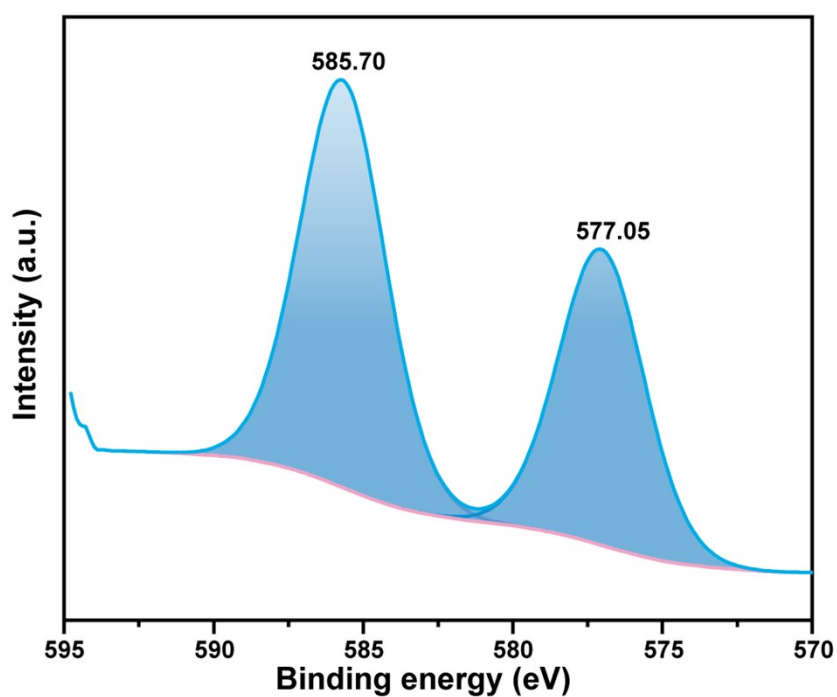
Figure S6. High-resolution Cr 2p XPS spectrum of **2Zn** after the Cr(VI) reduction cyclic experiment.
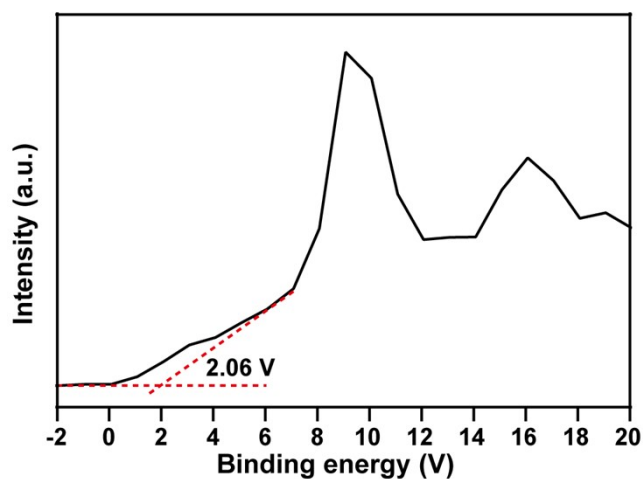
Figure S7. XPS valence band spectrum of **2Zn**.
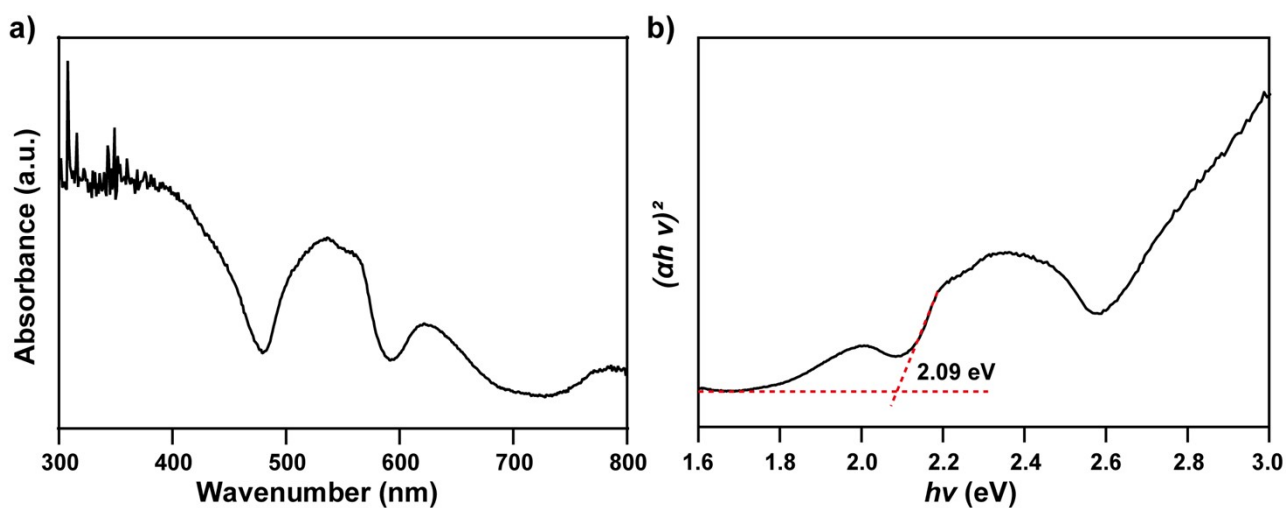
Figure S8. (a) Solid UV-visible absorption spectra of **2Zn**, (b) the band edges of **2Zn**.

Theoretical calculation

Method: All the calculations were carried out by the Gaussian16 package[S4]. The PBE0 hybrid functional[S5] was applied for all calculations. For geometry optimization, the mixed basis sets of SDD for Cr and 6-31G(d,p) for other atoms with SMD[S5] continuum solvent model with water as solvent were used. Analytical frequency calculations were performed at the same level of theory as the geometry optimization to identify the nature of all the stationary points being the minimum (no imaginary frequency). Time-dependent DFT were used to calculated the vertical excitation energies of photocatalysts and $Cr_2O_7^{2-}$.
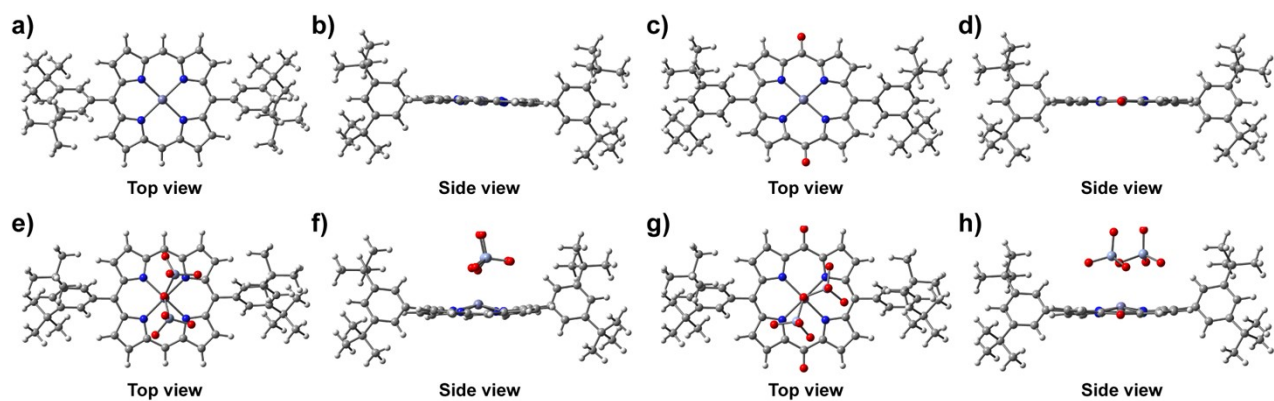
Figure S9. (a) (Top view) and (b) (Side view) Schematic representations of the optimized ground-state structure of photocatalyst **1Zn**；(c) (Top view) and (d) (Side view) Schematic representations of the optimized ground-state structure of photocatalyst **2Zn**；(e) (Top view) and (f) (Side view) Schematic representations of the adsorption of $Cr_2O_7^{2-}$ on photocatalyst **1Zn**；(g) (Top view) and (h) (Side view) Schematic representations of the adsorption of $Cr_2O_7^{2-}$ on photocatalyst **2Zn**.

Table S1

Comparison of reported literature on the photo-reduction of Cr(VI).

Photocatalyst	Catalyst dosage (mg)	Initial Cr(VI) concentration (mg/L)	Solution volume (mL)	Material type	Reduction efficiency (%) and capacity (mg/g)	Refs.
BCG-5	30	20	50	Composite material	81.51% 26.7/1	S6
ZnO/Bi_2S_3	50	20	50	Composite material	95% 19/1	S7
Carbon dots-TiO_2	50	10	50	Composite material	99.2% 9.9/1	S8
RGO/α-MnO_2	50	10	50	Composite material	76% 7.6/1	S9
Bi_2WO_6	60	10	50	Composite material	78% 6.5/1	S10
CoS_2	10	20	20	Composite material	10.2% 4.1/1	S11
CdS	30	10	150	Composite material	13% 6.5/1	S12
Bi_2O_3/Bi_2S_3	25	80	50	Composite material	91.8% 146.9/1	S13
CoS_2/g-C_3N_4-rGO	10	20	20	Composite material	72% 28.8/1	S14
2Zn	5	60	30	Homogenous material	75.6% 272.2/1	This study

References

[S1] M. j. Smith, L. M. Blake, W. Clegg, H. L. Anderson, *Org. Biomol. Chem.*, 2018, **16**, 3648-3654.

[S2] M. Umetani, T. Tanaka, T. Kim, D. Kim, A. Osuka, *Angew. Chem. Int. Ed.*, 2016, **55**, 8095-8099.

[S3] F. P. Zhao, Y. P. Liu, S. B. Hammoud, B. Doshi, N. Guijarro, X. B. Min, C. J. Tang, M. Sillanpääe, K. Sivulad, S. B. Wang, *Appl. Catal., B*, 2020, **272**, 119033.

[S4] M. J. Frisch, G. W. Trucks, H. B. Schlegel, G. E. Scuseria, M. A. Robb, J. R. Cheeseman, G. Scalmani, V. Barone, G. A. Petersson, H. Nakatsuji, X. Li, M. Caricato, A. V. Marenich, J. Bloino, B. G. Janesko, R. Gomperts, B. Mennucci, H. P. Hratchian, J. V. Ortiz, A. F. Izmaylov, J. L. Sonnenberg, Williams, F. Ding, F. Lipparini, F. Egidi, J. Goings, B. Peng, A. Petrone, T. Henderson, D. Ranasinghe, V. G. Zakrzewski, J. Gao, N. Rega, G. Zheng, W. Liang, M. Hada, M. Ehara, K. Toyota, R. Fukuda, J. Hasegawa, M. Ishida, T. Nakajima, Y. Honda, O. Kitao, H. Nakai, T. Vreven, K. Throssell, J. A. Montgomery, J. E. Peralta, F. Ogliaro, M. J. Bearpark, J. J. Heyd, E. N. Brothers, K. N. Kudin, V. N. Staroverov, T. A. Keith, R. Kobayashi, J. Normand, K. Raghavachari, A. P. Rendell, J. C. Burant, S. S. Iyengar, J. Tomasi, M. Cossi, J. M. Millam, M. Klene, C. Adamo, R. Cammi, J. W. Ochterski, R. L. Martin, K. Morokuma, O. Farkas, J. B. Foresman, Fox, D. J. Gaussian 16 Rev. A.03, Wallingford, CT, 2016.

[S5] A. V. Marenich, C. J. Cramer, D. G. Truhlar, *J. Phys. Chem. B* 2009, **113**, 6378-6396.

[S6] S. M. Ghoreishian, S. R. Ranjith, B. Park, S. K. Hwang, R. Hosseini, R. Behjatmanesh-Ardakani, S. M. Pourmortazavi, H. U. Lee, B. Son, S. Mirsadeghi, Y. K.

Han and Y. S. Huh, *Chem. Eng. J.*, 2021, **419**, 129530.

[S7] X. Y. Yuan, X. Wu, Z. J. Feng, W. Jia, X. X. Zheng, C. Q. Li, *Catalysts*, 2019, **9**, 624.

[S8] Y. R. Li, Z. M. Liu, Y. C. Wu, J. T. Chen, J. Y. Zhao, F. M. Jin, P. Na, *Appl. Catal., B*, 2018, **224**, 508-517.

[S9] D. k. Padhi, A. Baral, K. Parida, S. K. Singh, M. K. Ghosh, *J. Phys. Chem. C*, 2017, **121**, 6039-6049.

[S10] F. Xu, H. M. Chen, C. Y. Xu, D. P. Wu, Z. Y. Gao, Q. Zhang, K. Jiang, *J. Colloid Interface Sci.*, 2018, **525**, 97-106.

[S11] Y. J. Wang, S. Y. Bao, Y. Q. Liu, W. W. Yang, Y. S. Yu, M. Feng, K. F. Li, *Appl. Surf. Sci.*, 2020, **510**, 145495.

[S12] F. Deng, X. Y. Lu, Y. B. Luo, J. Wang, W. J. Che, R. J. Yang, X. B. Luo, S. L. Luo, D. D. Dionysiou, *Chem. Eng. J.*, 2019, **361**, 1451-1461.

[S13] Y. Sang, X. Cao, G. D. Dai, L. X Wang, Y. Peng, B. Y. Geng, *J. Hazard. Mater.*, 2020, **381**, 120942.

[S14] X. Zhang, W. W. Yang, M. Y. Gao, H. Liu, K. F. Li, Y. S. Yu, *Green, Energy Environ.*, 2022, **7**, 66-74.